912–923 *Nucleic Acids Research, 2020, Vol. 48, No. 2* *Published online 5 December 2019*
doi: 10.1093/nar/gkz1145

mRNA regions where 80S ribosomes pause during translation elongation *in vivo* interact with protein uS19, a component of the decoding site

Elena S. Babaylova[1,†], Alexander V. Gopanenko[1,†], Konstantin N. Bulygin[1], Alexey E. Tupikin[1], Marsel R. Kabilov[1], Alexey A. Malygin[1,2] and Galina G. Karpova[1,2,*]

[1]Institute of Chemical Biology and Fundamental Medicine, Siberian Branch of the Russian Academy of Sciences, Prospekt Lavrentieva 8, Novosibirsk 630090, Russia and [2] Novosibirsk State University, Pirogova Str. 2, Novosibirsk 630090, Russia

Received March 12, 2019; Revised November 21, 2019; Editorial Decision November 21, 2019; Accepted November 25, 2019

ABSTRACT

In eukaryotic ribosomes, the conserved protein uS19, formerly known as S15, extends with its C-terminal tail to the decoding site. The cross-linking of uS19 to the A site codon has been detected using synthetic mRNAs bearing 4-thiouridine (s^4U) residues. Here, we showed that the A-site tRNA prevents this cross-linking and that the P site codon does not contact uS19. Next, we focused on determining uS19-mRNA interactions *in vivo* by applying the photoactivatable-ribonucleoside enhancing cross-linking and immunoprecipitation method to a stable HEK293 cell line producing FLAG-tagged uS19 and grown in a medium containing s^4U. We found that when translation was stopped by cycloheximide, uS19 was efficiently cross-linked to mRNA regions with a high frequency of Glu, Lys and, more rarely, Arg codons. The results indicate that the complexes, in which the A site codon is not involved in the formation of the mRNA-tRNA duplex, are present among the cycloheximide-arrested 80S complexes, which implies pausing of elongating ribosomes at the above mRNA regions. Thus, our findings demonstrate that the human ribosomal protein uS19 interacts with mRNAs during translation elongation and highlight the regions of mRNAs where ribosome pausing occurs, bringing new structural and functional insights into eukaryotic translation *in vivo*.

INTRODUCTION

The final stage of the implementation of genetic information is the synthesis of proteins, one of the most important cellular processes. In all kingdoms of life, this process occurs on ribosomes, where the information, copied from DNA and encoded as trinucleotide (codon) sequences in mRNAs, is translated into the amino acid sequences of the synthesized proteins. The interaction of the ribosome with mRNA and tRNA, which occurs with the help of auxiliary protein factors, is a central event at all stages of translation. Currently, the structural organization of key functional centers of ribosomes, including the mRNA binding channel, where codon-anticodon interactions take place, is well known. Remarkably, rRNA nucleotides involved in the formation of this channel on the small subunit form a conserved core, which is structurally identical in bacterial and eukaryotic ribosomes (reviewed in (1)). In addition, some conservative features of the mRNA channel are provided by the ribosomal proteins uS3, uS7, uS11 and uS12 (reviewed in (1,2)). However, with all this, there are also significant differences in the protein environments of mRNAs on bacterial and eukaryotic ribosomes. These differences relate to the participation of ribosomal proteins eS30, eS26 and eS28, which do not have bacterial homologues, as well as the eukaryote/archaea-specific extension of the uS19 protein in the formation of the mRNA binding channel of eukaryotic ribosomes (reviewed in (1)). It should be noted that ribosomal proteins are named here according to the nomenclature proposed in (3).

The protein uS19 (previously named S15 (see 3)) has first been identified as a component of the decoding site of mammalian ribosomes by affinity cross-linking using mRNA analogues containing the 4-thiouridine (s^4U) residue at a certain position (4–6). In these reports, the contact of the 19 kDa ribosomal protein with the s^4U residue at any position of the A-site codon has been shown in the absence of a ligand at the A site. A little later, the data that uS19 is a characteristic component of the ribosomal decoding site, have also been obtained using mRNA analogues carrying a photoactivatable aryl azide group at the nucleotide in a definite

*To whom correspondence should be addressed. Tel: +7 383 363 5140; Fax: +7 383 363 5153; Email: karpova@niboch.nsc.ru
†The authors wish it to be known that, in their opinion, the first two authors should be regarded as Joint First Authors.

position (7–9). After some time, the participation of uS19 in the formation of the decoding center of mammalian ribosomes has again been confirmed by means of the same approach using synthetic mRNAs containing the s^4U residue at a certain location (10,11) as well as mRNA analogues with oxidized 3′-terminal ribose (12). In addition, studies on the cross-linking of human ribosomes to mRNA analogues have revealed that the protein eS30 is also a component of the decoding site (7–9,12). According to cryo-electron microscopy (cryo-EM) data (13), the expanded and poorly structured eS30 interacts with the A site region through its N-terminal fragment. This part of eS30 has been shown to cross-link to an mRNA analogue with oxidized 3′-terminal ribose at position +7 relative to the first nucleotide of the P site-bound codon (14). As for uS19, using the cross-linking of human ribosomes to photoactivatable mRNA analogues followed by site-directed cleavage of cross-linked uS19 with proteolytic agents, it has been found that the C-terminal unstructured tail of the protein, namely its fragment 131–145, is involved in the interaction with the nucleotide bases of the A site codon (15).

Much later, the C-terminal tail of uS19 has been localized in the 40S ribosomal decoding area using cryo-EM, and some assumptions about interactions of this protein with mRNA and tRNA have been made (16). In particular, it has been suggested that the uS19 tail interacts with the A and P site tRNA anticodon stem-loops rather than with mRNAs, without taking into account the data of numerous cross-linking studies mentioned above, which had clearly demonstrated that this tail interacts with the A site mRNA codon. Moreover, according to these studies, the uS19 tail is able to interact with the A site codon in various types of ribosomal complexes that correspond to different translation steps, from the start codon recognition up to the appearance of a stop codon at the A site (reviewed in (1)). In addition, it has been shown that the appearance of a ligand at the A site can completely block the cross-linking of an mRNA analogue to uS19. In particular, the binding of eRF1 interferes with the cross-linking of uS19 to a synthetic mRNA containing the s^4U residue in the stop codon (4–7), and tRNA prevents the interaction of the protein with an mRNA analogue with 3′-oxidized ribose (12,14).

Now, it has become possible to find out whether the ribosomal protein uS19 is indeed involved in the translation process, using the photoactivatable-ribonucleoside enhancing cross-linking and immunoprecipitation (PAR-CLIP) approach, which allows the transcriptome-wide determination of RNA binding protein interaction sites. In this study, we applied the PAR-CLIP method to a specially designed stable cell line, inducibly producing human ribosomal protein uS19 with an N-terminal FLAG-tag (^{FLAG}uS19), which was able to functionally replace the endogenous uS19 in the ribosomes. RNA-protein cross-links were generated in the cells that were grown in a medium containing s^4U and treated with cycloheximide that binds to the ribosome in the E site pocket on the large subunit and thereby blocks the translocation of tRNA from the P site to the E site (17–19). Therefore, in the cycloheximide-arrested ribosomes, the A site should be occupied by peptidyl-tRNA, which could protect uS19 from cross-linking to the mRNA codon containing the s^4U residue in accordance with the above data on shielding the protein by the A-site-bound ligand. However, given the possible pausing of ribosomes during translation elongation (20,21), we expected that this treatment would lead to the appearance of complexes with different peptidyl-tRNA states, including those, in which the A site codon did not participate in the formation of the mRNA-tRNA duplex and could interact with ^{FLAG}uS19. Next generation sequencing (NGS) of cDNA libraries derived from cross-linked RNA fragments revealed several hundreds of the clusters of sequencing reads with characteristic T/C transitions indicating, according to (22), s^4U-dependent cross-linking of cellular RNAs to ^{FLAG}uS19. To correctly interpret the PAR-CLIP results, we performed *in vitro* experiments on cross-linking human ribosomes to mRNA analogues containing s^4U residues, which confirmed that interaction with uS19 is indeed a characteristic feature of the A site mRNA codon and that the A site tRNA interferes with this interaction. Mapping the positions of T/C transitions to the human genome showed that detected read clusters correspond to coding sequence (CDS) regions of mRNAs with a high frequency of Glu, Lys and, more rarely, Arg codons. This meant that the ribosomes were already paused at these regions before the translation was stopped by cycloheximide, and that the A site codon was not involved in the formation of the mRNA-tRNA duplex in the paused ribosomes, which allowed this codon to cross-link to ^{FLAG}uS19 if it contained the s^4U residue. Thus, the obtained results revealed previously unknown features of the translation elongation process in mammalian cells, demonstrating the involvement of the ribosomal protein uS19 in maintaining the proper location of the mRNA codon at the decoding site and displaying mRNA regions, the reading of which causes ribosome pausing.

MATERIALS AND METHODS

Affinity cross-linking of s^4U-containing mRNA analogues to human ribosomes

Human ribosomal 40S and 60S subunits were isolated from full term placenta, as described in (23). Purified $tRNA^{Phe}$ (∼80%) and $tRNA^{Val}$ (∼70%) from *Escherichia coli* were the kind gifts from Dr V.I. Katunin (St. Petersburg Nuclear Physics Institute named by B.P. Konstantinov of National Research Center 'Kurchatov Institute', Gatchina, Russia). Yeast $tRNA^{Asp}$ transcript was obtained by T7 transcription *in vitro*, as described (24). DNA templates for the synthesis of mRNA analogues with randomly distributed s^4U residues by T7 transcription *in vitro* were obtained by hybridization of the following oligodeoxyribonucleotide pairs: F-Asp, 5′-aaattaatacgactcactatagggaagaaagaagataaagaaaaagaa-3′ and R-Asp, 5′-ttctttttctttatcttctttcttccctatagtgagtcgtattaattt-3′; F-PheAsp, 5′-aaattaatacgactcactatagggaagaaagaattcgataaagaaaaa-3′ and R-PheAsp, 5′-tttttctttatcgaattctttcttccctatagtgagtcgtattaattt-3′; F-PheVal,

5′-aaattaatacgactcactatagggaagaaagaattcgtaaaagaaaaa-3′ and R-PheVal, 5′-tttttcttttacgaattctttcttccctatagtgagtcgt attaattt-3′; F-PheVal(C-rich), 5′-cgattaatacgactcactatag ggaagccaccattcgtacaccaccac-3′ and R-PheVal(C-rich), 5′-gtggtggtgtacgaatggtggcttccctatagtgagtcgtattaatcg-3′.
The T7 transcription reaction was carried out as described (25); the concentrations UTP and s^4UTP in reaction mixture were 0.5 mM. After the reaction, the synthesized RNAs were purified by 12% denaturing PAGE and used as mRNA analogues. There were 5′-GGGAAGAAAGAAGAs^{4}UAAAGAAAAAGAA-3′, 5′-GGGAAGAAAGAAs^{4}Us^{4}UCGs^{4}UAAAAGAAAA A-3′, 5′-GGGAAGAAAGAAs^{4}Us^{4}UCGAs^{4}UAAAGA AAAA-3′ and 5′-GGGAAGCCACCAs^{4}Us^{4}UCGs^{4}UA CACCACCAC-3′ designated hereinafter as mRNA I, II, III and IV, respectively. If necessary, the mRNAs and tRNAs were 5′ end dephosphorylated with FastAP alkaline phosphatase (Thermo Scientific) and then 5′ end ^{32}P-labeled in reaction with [γ-^{32}P]ATP and T4 polynucleotide kinase. Complexes of 80S ribosomes with mRNAs and tRNAs with codon-anticodon interactions either at the P site or at the P and A sites simultaneously, were obtained according to (12). The levels of binding to 80S ribosomes of ^{32}P-labeled $tRNA^{Asp}$ or $tRNA^{Phe}$ cognate to an mRNA triplet targeted to the P-site to form a ternary complex or to the A site to convert the latter into a quaternary one, and of the respective ^{32}P-labeled mRNAs were measured by nitrocellulose filtration assay as described (12). For cross-linking in the ternary complexes with mRNAs I-IV, reaction mixtures included 80S ribosomes (0.83 μM), ^{32}P-labeled mRNA (2 μM), and the tRNA (7 μM) in 50 mM Tris–HCl (pH 7.5) containing 100 mM KCl, 13 mM $MgCl_2$ and 0.5 mM EDTA (buffer A). For cross-linking in the quaternary complexes with mRNAs II and III, the respective reactive mixtures were supplemented with the appropriate tRNA to its concentration of 13 μM. After incubation under binding conditions (12), the above mixtures were irradiated with mild UV light (λ > 300 nm) (26), followed by analysis of cross-linked ribosomal proteins in 12% SDS PAGE as described (12). The identification of the cross-linked ribosomal proteins was carried out based on the retardation effect of the cross-linked RNA fragments on the electrophoretic mobility of ribosomal proteins known from our previous works (e.g. see (7–9,12,14)).

Cells culturing and transfection

The minigene of ^{FLAG}uS19 amplified with the use of HEK293 cDNA and primers F (5′-acgtgaattcatggtggacta caaagacgatgacgacaaggcagaagtagagcagaag-3′) and R (5′- ac gtgaattcttacttgagagggatgaagc-3′) was inserted into pAG-1 vector (26) at EcoRI site in the forward direction. The resulting plasmid pAG-1(^{FLAG}uS19) was linearized by BamHI and then utilized to transfect HEK293 cells (ATCC CRL-1573) using Lipofectamin LTX (Invitrogen). The selection of cell clones stably producing the target protein was performed as described (26). Stable clones were tested for their ability to produce ^{FLAG}uS19 after doxycycline (DOX) induction by western blotting using anti-FLAG M5 (Sigma, #F4042) as described (26).

PAR-CLIP analysis of a stable cell line producing ^{FLAG}uS19

The PAR-CLIP procedure was carried out according to (22) with some modifications in three biological replicates. Typically, adherent pAG-1(^{FLAG}uS19)-derivatized HEK293 cells in four 15-cm Petri dishes were cultured in Dulbecco's modified Eagle's medium (DMEM) containing 10% FBS and 100 U/ml of Penicillin–Streptomycin (all from Thermo Fisher Scientific) in CO_2-incubator (5% CO_2) at 37°C. At 60–70% confluency, the production of ^{FLAG}uS19 in cells was induced with DOX (2 μg/ml) and after 44 h, s^4U was added to 250 μM. After 6 h, cycloheximide was added to a concentration of 100 μg/ml and the cells were kept on ice for 10 min, followed by washing with ice-cold PBS. Cross-linking was performed by irradiation of the cells with UV light at 365 nm (0.5 J/cm^2) in Bio-Link (Vilber Lourmat) on ice. In the control experiment, s^4U was not added to the cell medium and the cells were not UV-irradiated. Finally, the cells were harvested with ice-cold PBS and centrifuged at 1000 g.

The cell pellet was lysed in three volumes of lysis buffer (20 mM Tris–HCl (pH 7.5), 150 mM NaCl, 5 mM $MgCl_2$, 1mM DTT, 1% Triton-X100, 100 μg/ml of cycloheximide and 0.02 U/μl of Turbo DNase I (Ambion)) for 10 min on ice and then triturated through 29 G needle 10 times. The cell lysate was clarified by centrifugation at 20 000 g for 15 min at 4°C and the supernatant was transferred into a new Eppendorf tube. RNase I (Ambion) was added to 1.3 U/μl, and the reaction mixture was incubated at ambient temperature for 45 min, followed by the addition of SUPERase In RNase inhibitor (Thermo Fisher Scientific) to 0.35 U/μl. The mixture was then clarified as described above, and the supernatant (∼750 μl) was layered onto 1 ml of 30% sucrose cushion (containing 20 mM Tris–HCl (pH 7.5), 150 mM NaCl, 5 mM $MgCl_2$, 1 mM DTT, 1% Triton-X100, 100 μg/ml of cycloheximide and 0.02 U/μl of SUPERase In) in a SW60 rotor centrifuge tube. Free tube volume was supplemented with 20 mM Tris–HCl (pH 7.5) buffer containing 150 mM NaCl, 5 mM $MgCl_2$ and 1 mM DTT, and the tube was centrifuged in SW60 Ti rotor at 25 000 rpm for 16 h at 4°C. The pellet was dissolved in 10 mM ethylenediaminetetraacetic acid (EDTA) containing 1% SDS, incubated for 30 min at 37°C and then diluted 20-fold with IP buffer (20 mM Tris–HCl (pH 7.5), 150 mM NaCl, 0.1% Nonidet P40 and protease inhibitor cocktail (Sigma)). The mixture was clarified as described above, and anti-FLAG M2 antibodies (Sigma, #F1804) bound to magnetic Protein G beads (Dynabeads, Life Technologies) were added to the supernatant. Typically, 10 μg of antibodies were bound to 40 μl of Dynabeads in one experiment as described (26). Immunoprecipitation was carried out for 3 h at 4°C on a rotating platform and the supernatant was then removed. The beads were washed with 1 ml of IP buffer (50 mM Tris–HCl (pH 7.5), 300 mM NaCl, 0.05% Nonidet P40 and 0.5 mM DTT), three times with 1 ml of HS buffer (50 mM Tris–HCl (pH 7.5), 500 mM NaCl, 0.05% Nonidet P40 and 0.5 mM DTT) and twice with 1ml of Defos buffer (50 mM Tris–HCl (pH 7.5), 100 mM NaCl, 10 mM $MgCl_2$ and 1 mM DTT). The remaining procedures, including the dephosphorilation of RNA fragments cross-linked to ^{FLAG}uS19, their 5′-end labeling with [γ-^{32}P]ATP and phosphorylation with ATP

as well as cross-link separation by SDS-PAGE followed by transfer onto the nitrocellulose membrane and the isolation of cross-linked RNA fragments, were carried out as described (26).

NGS sequencing, data processing and bioinformatics analysis

DNA libraries were prepared according to (27) and sequenced with 2 × 75 bp paired-ends reagents on MiSeq (Illumina) in SB RAS Genomics Core Facility (Institute of Chemical Biology and Fundamental Medicine, SB RAS, Novosibirsk, Russia). Reads were demultiplexing by CEL-Seq script (28). Adapter and low-quality sequences were removed using TrimGalore v.0.5.0 software (http://www.bioinformatics.babraham.ac.uk/projects/trim_galore). Read mapping was performed against the Ensembl annotated human genome (GRCh38.93) with STAR v.2.6.1 software (29). BAM deduplication by unique molecular indexes was carried out with 'dedup' script from UMI-tools (30). Transitions were found by Basic Variant Detection in CLC GW v.12.0 software (Qiagen) and filtered by custom python scripts. The read data reported in this study were submitted to the GEO under the accession number GSE128265.

The uS19 cross-linking sites were detected by the appearance of characteristic T/C (for plus DNA stands) and A/G (for minus DNA strands) transitions in the sequencing reads, which were found as described above, with parameters: minimum coverage, 5; minimum count, 1; minimum frequency, 1%. The resulting variant call format (VCF) files were used for subsequent downstream analysis that was carried out using R Bioconductor platform packages. Genomic positions from VCF files were used as coordinates of cross-linking sites and were annotated by ensembl transcript IDs and HGNC gene symbols using 'biomaRt' package (31) and Ensembl annotation GRCh38.93. Coordinates of transitions that corresponded to the non-protein coding part of the genome and the mitochondrial genome, were removed from the main part of the subsequent analysis. Genomic positions were transformed to internal CDS coordinates according to Ensembl annotation GRCh38.93. The resulting peaks were identified using the 'chipseq' and 'coverage view' packages and were matched with the positions of the above-mentioned transitions. Only peaks overlapping with transition positions and having coverage above the threshold were considered as read clusters. Among the transition positions that corresponded to a particular cluster, only the position with the highest T/C transition coverage was considered as the main cross-linking site, where appropriate.

CDS sequences were downloaded from Ensembl (www.ensembl.org/info/data/ftp/Homo_sapiens.GRCh38.cds.all.fa) and subsequences from –19 triplet upstream to +19 triplet downstream of the transition internal CDS coordinate were extracted. Considering the open reading frames, the resulting sequences were translated into amino acid sequences that were used for the LOGO analysis utilizing the Weblogo tool (https://weblogo.berkeley.edu/). The read clusters were sorted based on the total cluster read coverage, and the transition context LOGOs were created for all found clusters, including the 100 most covered ones ('top100'). Histograms and graphics were built using integrated R tools.

The correlation between PAR-CLIP replicates was measured using the standard R function (cor), and the resulting plots were generated using the ggplot2 package. To compare the raw reads to each other, read count correlation tables were generated using the summarizeOverlaps function with the default parameters from the GenomicAlignment package (32). For all identified clusters, the total coverage was estimated using the CoverageView package, and then applied to correlation measurements.

To find proteins with $(E/K)_{12}$ motifs, a set of all human protein sequences was recovered from Ensembl (https://www.ensembl.org/info/data/ftp/). The amino acid sequences were scanned for the presence of any of the 2^{12} $(E/K)_{12}$ motifs using the Bioconductor Biostrings package with the vcount-Pattern function with the max.mismatch parameter equal to 4 and other parameters default.

Ribosome profiling with cells producing ^{FLAG}uS19 and cells grown in a medium containing s^4U

For ribosome profiling with HEK293 cells producing ^{FLAG}uS19, pAG-1(^{FLAG}uS19)-derivatized HEK293 cells were grown in three biological replicates as in the PAR-CLIP experiment. For the same task with HEK293 cells grown in the presence of s^4U, the cells were cultured in 10-cm Petri dishes as described above in three biological replicates up to 60% confluency, and then s^4U was added to one half of the Petri dishes up to 250 μM, followed by incubation for 16 h and the cells collection. Subsequent manipulations, including cell lysis, RNase I treatment of the lysate and its centrifugation through a sucrose cushion were the same as described above. With HEK293 cells producing ^{FLAG}uS19, the resulting pellet was solubilized in 200 μl of buffer A and incubated with 15 μl of Protein G beads pre-bound with anti-FLAG M2 antibodies for 3 h at 4°C followed by separation of the supernatant from the beads. Total RNA was isolated from the supernatant fraction containing ribosomes with endogenous uS19 and from ribosomes remaining on beads and containing uS19^{FLAG} using TRIzol (Ambion) according to the manufacturer's protocol. Total RNA from ribosomal pellet obtaining after centrifugation of the cell lysate through a sucrose cushion in the experiment with HEK293 cells grown in the presence of s^4U was isolated in the same way. Subsequent procedures, including RNA fragments size selection and purification, were performed according to (33). DNA libraries were prepared and sequenced as above. The corresponding Ribo-seq data were submitted to the GenBank under the study accession PRJNA563539 and the sample accession SRP220276.

RESULTS

Verification of cross-linking of uS19 to mRNA analogues carrying the s^4U residue in the codon directed to the ribosomal A or P sites

To make sure that the protein uS19 really interacts only with the A-site mRNA codon and that the A-site-bound tRNA

interferes with this interaction, we performed experiments on the affinity cross-linking of human ribosomes to synthetic mRNAs I-IV bearing s^4U residues (Supplementary Figure S1). When designing sequences of the mRNAs, we took into account that the s^4U residue in the second position of the P site codon does not form cross-links with uS19, unlike the one located in the same position of the A site codon (10,11). Thus, in the resulting ribosome complexes with the mRNAs, the s^4U residue was either at positions +2 or +3 (complex 1), or positions +5 or +6 (complexes 2–6) relative to the first nucleotide of the P site-bound codon, which corresponds to the location of the s^4U-containing triplet at the P or A site, respectively. In complexes 1–3 and 6, the A site was empty, and in complexes 4–5 it was occupied by tRNA cognate to the codon bound there. All mRNAs used were able to efficiently bind to ribosomes in the presence of $tRNA^{Asp}$ or $tRNA^{Phe}$, which directed the cognate codon to the P site (Supplementary Figure S1A, left panel). Analysis of proteins isolated from irradiated complex 1–6 showed that the cross-linking patterns generated by mRNA I-IV contain the ones similar to those observed for the respective binary mixtures, where the mRNAs were not fixed on the ribosomes by the codon-anticodon interaction at the mRNA-binding channel (Supplementary Figure S1, right panels). These common patterns correspond to the uS3 and eS30 proteins cross-linked to mRNA I–IV through specific structural motifs lying outside the 40S subunit channel, which are known to cross-link to mRNA analogues loosely coupled to ribosomes in the absence of tRNA (12,14). The appearance of cross-linked uS3 and eS30 in all the patterns in not surprising, since labile binary complexes of mRNA analogues with ribosomes are usually present in the corresponding reaction mixtures, along with those in which the mRNA analogue is fixed in the channel (12,14).

As expected, in complexes 2, 3 and 6, uS19 was cross-linked to the s^4U residue at positions +5 or +6, unlike complex 1, where cross-linking to uS19 did not occur. The levels of cross-linking of mRNAs II and III to uS19 in complexes 4 and 5 were reduced by more than 40% compared to those in complexes 2 and 3 (Supplementary Figure S1B, right panel), which indicates the shielding effect of the A site tRNA. This value becomes even higher if we take into account that in complexes 4 and 5, up to a third of 80S ribosomes can have the empty A-site, as follows from a comparison of the isotherms of tRNA binding in the A and P sites (see Supplementary Figure S1A and B). It is noteworthy that the cross-linking patterns obtained for complexes 2 and 3 with mRNAs II and III, respectively, rich in purine bases, were identical to that for similar complex 6 with mRNA IV rich in pyrimidine ones (Supplementary Figure S1B and C), indicating that the nucleotide context around the A site codon does not affect its contact with uS19. Thus, we conclude that uS19 is a specific target for the s^4U residue at any position of the A site codon, which is unattainable for the one at the third position of the P site codon, and that uS19 becomes significantly less accessible for the cross-linking if the A site codon is involved in interaction with a cognate tRNA.

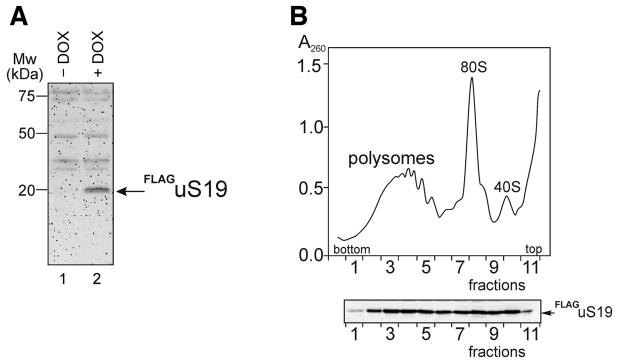

Figure 1. The production of ^{FLAG}uS19 in transfected HEK293 cells and the incorporation of the protein into the ribosomes. (**A**) Western blot analysis of ^{FLAG}uS19 production in the cells induced by DOX (+DOX) and without the induction (−DOX) using antibodies against FLAG-peptide. The positions of molecular weight markers are indicated on the left. (**B**) The sedimentation profile of ^{FLAG}uS19-producing cell lysate in a sucrose gradient (upper panel) and Western blot analysis of the content of ^{FLAG}uS19 in gradient fractions (lower panel). Gradient fractions are numbered from the bottom to top.

Characterization of the used stable cell line and in-cell RNA cross-linking

To study the contacts of human ribosomal protein uS19 with translated mRNAs using the PAR-CLIP method, we designed an appropriate stably transfected cell line based on HEK293 cells. A plasmid utilized to transfect cells was obtained using a previously developed mammalian expression vector (26) with a cloned DNA insert encoding ^{FLAG}uS19, which allowed this protein to be produced in the transfected cells in response to the induction with doxycycline (DOX) (Figure 1A). To validate the functionality of ^{FLAG}uS19 produced by the above stable cell line, we performed polysome profiling of the cell lysate in a sucrose density gradient, followed by western blot analysis of the respective fractions for the target protein content. The ribosome and polysome fractions were shown to contain ^{FLAG}uS19, which implies that the N-terminal FLAG epitope does not significantly affect the functions of the uS19 protein in ribosomes (Figure 1B).

To ensure that neither the presence of FLAG-tagged uS19 in ribosomes, nor the incorporation of s^4U in mRNAs affect the profile of translated mRNAs, we performed two series of control experiments on ribosome profiling (34). In particular, we compared the profiles of mRNAs translated by ribosomes containing endogenous uS19 and by ^{FLAG}uS19-containing ones, as well as the profiles of mRNAs translated in s^4U-treated and untreated cells. In both the first and second series of control experiments, we found a high correlation between the corresponding datasets (Supplementary Figure S2); Pearson's coefficients were 0.96 and 0.85, respectively. This means that the PAR-CLIP method utilizing s^4U can be applied to cells ectopically producing ^{FLAG}uS19 to detect contacts of mRNAs with this protein during translation *in vivo*. In addition, it should be noted that in the original article on PAR-CLIP (22), it has been mentioned

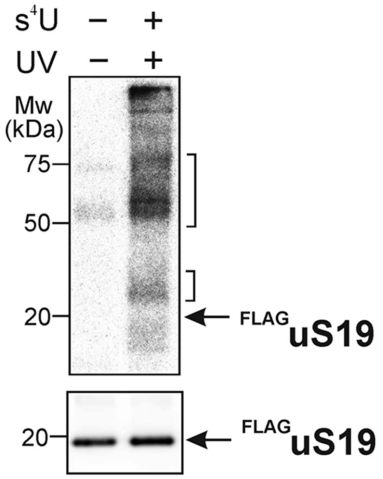

Figure 2. In-cell s^4U-enhanced ^{FLAG}uS19 cross-linking and immunoprecipitation. Autoradiogram of the membrane with ^{FLAG}uS19 cross-linking products immunoprecipitated with antibodies against FLAG-epitope and resolved by SDS-PAGE (upper panel). Upper and lower groups of cross-links are marked on the right. Western blot analysis of the same membrane with anti-FLAG antibodies is shown in the lower panel. Arrows indicate position of ^{FLAG}uS19. The positions of molecular weight markers are indicated on the left.

that s^4U does not have significant cytotoxicity when added to the cell medium up to a final concentration of 1 mM.

In-cell RNA cross-linking, along with all subsequent procedures, was performed in accordance with the PAR-CLIP protocol (22), which included elements of the ribosome profiling one (34). Briefly, DOX-induced cells grown to 80–90% confluency were treated with s^4U and, after stopping the translation by cycloheximide, were irradiated with mild UV light (365 nm) to induce the formation of cross-links. After cell lysis, the fraction containing the polysomes was treated with RNase I to cleave the mRNA regions uncovered by ribosomes. The resulting monosomes, including those containing mRNA fragments cross-linked to ^{FLAG}uS19 in the mRNA binding channel, were collected by sedimentation through a sucrose cushion and dissociated using SDS and EDTA. After ^{FLAG}uS19 immunoprecipitation using anti-FLAG antibodies, RNA fragments cross-linked to the protein were labeled with ^{32}P, and the respective RNA-protein cross-links were resolved by SDS-PAGE, followed by transfer onto a nitrocellulose membrane (Figure 2). Two major groups of ^{32}P-labeled RNA-protein cross-links migrating in the gel slower than ^{FLAG}uS19 were eluted from the membrane separately after proteinase K treatment, and cDNA libraries derived from RNA fragments corresponding to these groups of cross-links were subjected to NGS.

Analysis of NGS-derived data

In total, six cDNA libraries obtained from the upper and lower groups of RNA fragments cross-linked to ^{FLAG}uS19 (Figure 2), each in three biological replicates, were sequenced. A comparison of the datasets obtained for these replicates revealed a high correlation in raw read counts between them ($0.727 \leq r \leq 0.795$ for the upper group and $0.694 \leq r \leq 0.821$ for the lower group) (Supplementary Figure S3A), and therefore the respective datasets were combined. Mapping of sequencing reads to the human genome showed that they were mainly grouped into specific clusters. Many reads in these clusters contained characteristic T/C transitions, which are usually introduced by reverse transcriptase when it meets cross-linked s^4U residues (22). A cluster was considered as corresponding to a ^{FLAG}uS19 cross-linking region in mRNA, if overlapping sequencing reads within it covered at least one position with the T/C transition (or the A/G one for the genes located on the minus DNA strand). In addition, it was taken into account that (i) one T position was covered by at least two reads with T/C transitions, (ii) the total read coverage by the T/C transitions was $\geq$5 and (iii) the total T/C transition frequency was more than 1%. Given all this, we mapped to the human genome 2256 and 565 T/C transition positions corresponding to the upper and lower groups of RNA fragments cross-linked to ^{FLAG}uS19 (Figure 2), respectively. Since these sets of T/C transition positions overlapped with each other by 440 positions, and correlation in the read coverage per peak with transitions between them was high ($r = 0.859$) (Supplementary Figure S3B and C), we combined the datasets obtained with the cDNA libraries for the upper and lower groups of RNA fragments. As the result, read clusters with T/C transitions were assigned to 580 unique protein-coding genes (Supplementary Tables S1 and S2), where they almost completely fell into the regions corresponding to the CDSs of mRNAs transcribed from these genes, which could cross-link to ^{FLAG}uS19 only when they were in the ribosomal mRNA-binding channel. As a rule, the above clusters covered only certain parts of the CDSs (Figure 3 and Supplementary Figure S4). The length of these parts was different and could be up to several hundred nucleotides, although most of them were 30–100 nt long (Supplementary Figure S5). It should be noted that, when mapped to CDSs of mRNAs, the read clusters obtained in the PAR-CLIP experiment mainly overlap with those obtained in the ribosome profiling one, but the latter are distributed over all CDS lengths, whereas the former are located only in some regions of CDSs (see Supplementary Figure S6, and S2C and D, the bottom panels). As for the T/C transitions in the gene regions corresponding to the anticodon stem–loops of tRNAs, whose interactions with the uS19 tail had been suggested for tRNA molecules bound at the A and P sites in the cryo-EM study mentioned in the Introduction (16), they were not detected. However, the lack of T/C transitions in these regions could be due to reverse transcriptase stops during cDNA library preparation caused by the presence of hypermodified bases in the vast majority of tRNAs.

Analysis of mRNA sites cross-linked to ^{FLAG}uS19

Since *in vitro* uS19 is cross-linked to model mRNAs only when the s^4U residue is in the triplet located at the A site, we had every reason to believe that the codon in the open reading frame of a gene, to which a T/C transition is mapped, corresponds to the A site mRNA triplet cross-linked to ^{FLAG}uS19, and the T/C transition position conforms to that of the cross-linked s^4U residue in this triplet. Inspection of the nucleotide sequences in gene regions covered with reads

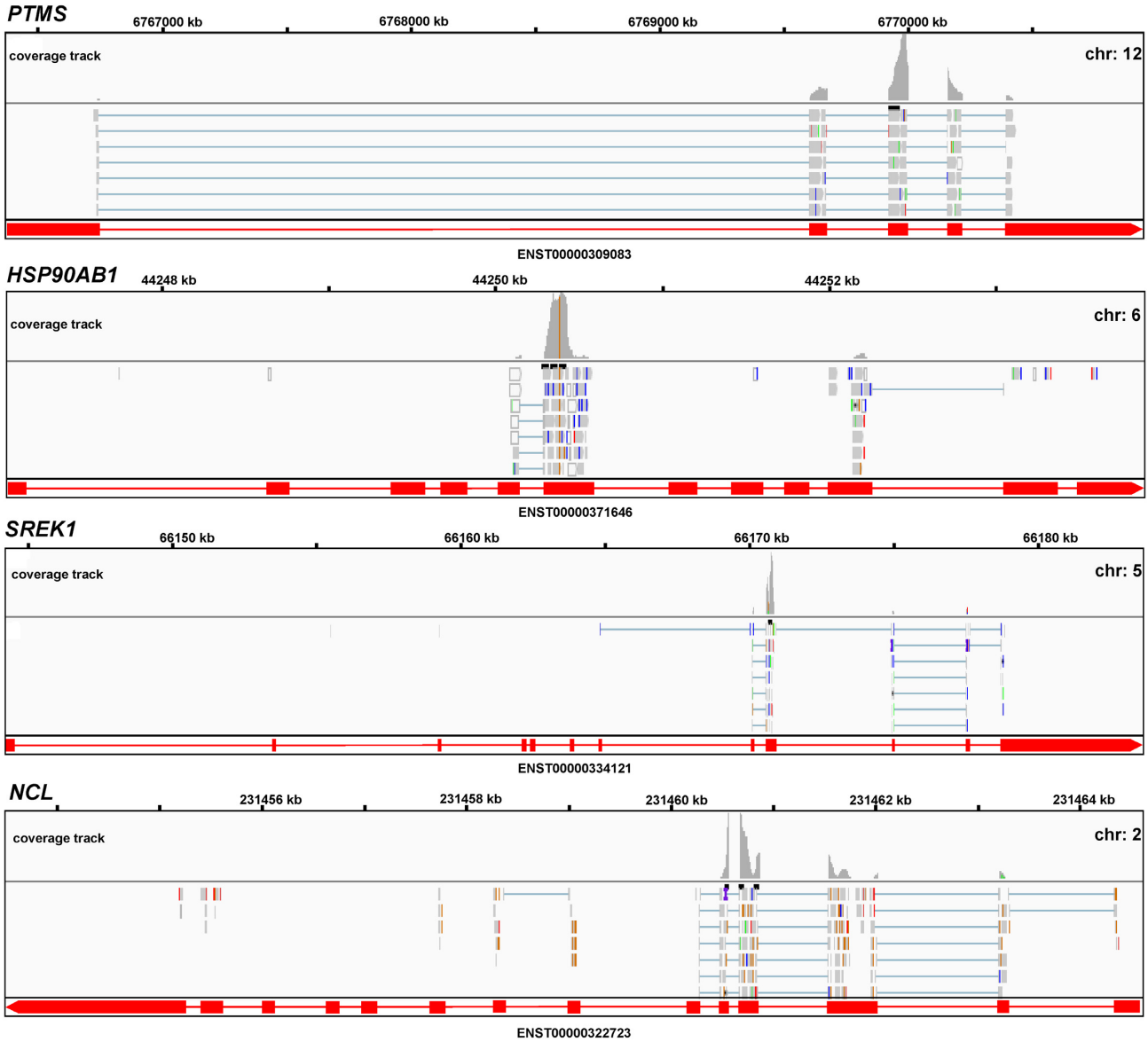

Figure 3. Localization of ^{FLAG}uS19 cross-linking sites. The IGV genome browser views of four representative genes with clusters of sequencing reads aligned to the human genome are shown. Exon/intron structures of the genes and the Ensembl IDs of their corresponding transcripts are presented in red below the browser panels. Coverage tracks show the location of peaks (gray histograms) representing the density of reads mapped to respective positions in exons.

containing T/C transitions showed that these sequences were enriched in residues G and A in the parts located both before and after the T/C transition positions (Figure 4). Moreover, this tendency was most pronounced for the gene regions revealed for the first hundred clusters with the highest read coverage (Figure 4). This implied that ^{FLAG}uS19 cross-linking occurred only to G/A-rich regions in CDSs of mRNAs. It should be noted that read clusters mainly fell only into those gene regions, where T residues were present and their positions precisely matched the T/C transition ones, and were practically not detected in regions that did not contain T residues (Figure 5), confirming that ^{FLAG}uS19 cross-linking to mRNAs was indeed s^4U-dependent. The T/C transitions in the sequencing reads were distributed so that the respective interaction sites in the mRNAs were in both 5′- and 3′-parts of the G/A-rich regions (Supplementary Figure S7). Since up to 28–34 nt could be accommodated at the ribosomal channel (35,36), these mRNA regions could be simultaneously covered with several closely stacked ribosomes. Analysis of the T/C transition positions in the sequencing reads showed that ^{FLAG}uS19 was able to cross-link to the s^4U residue located at any position of the A site mRNA codon, although the third position was more preferable since more than half of the T/C transition positions corresponded to cross-linking of the protein to s^4U in third position (Supplementary Figure S8). The latter, apparently, reflected the more frequent appearance of codons with the U residue in the third position as compared with codons with the ones in other positions in mRNAs that turned out to be cross-linked to uS19.

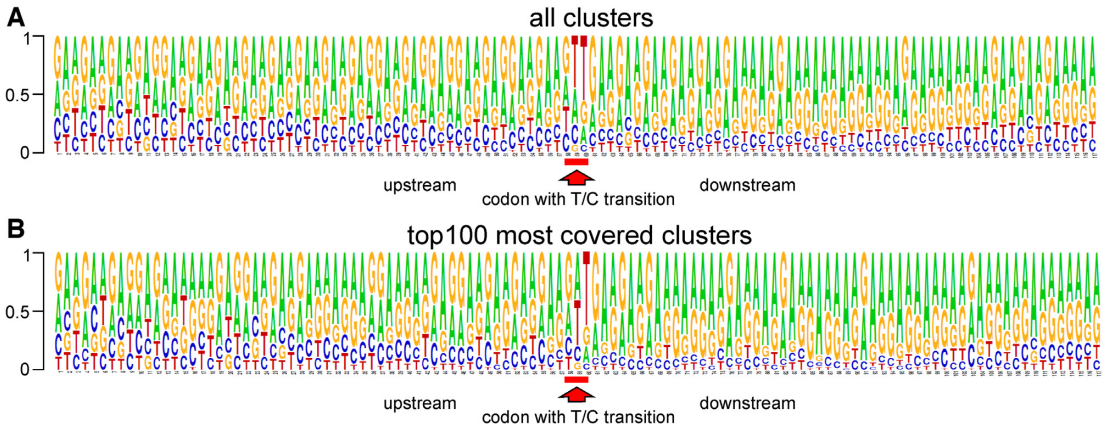

Figure 4. Logos of nucleotide sequences covered with read clusters with T/C transitions and aligned to sequences consisting of the codon, in which the T/C transition is detected, and of 19 nucleotide triplets upstream and downstream of it. (**A**) Logo for all found read clusters, and (**B**) logo for the top 100 most read-covered clusters.

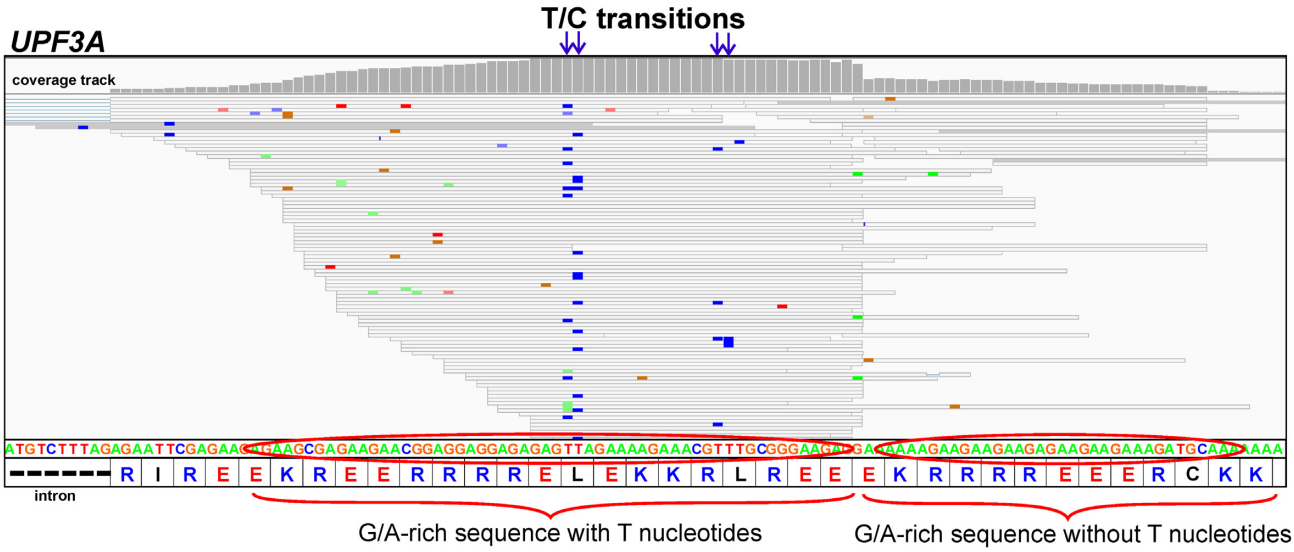

Figure 5. The IGV genome browser view of the cluster of sequencing reads aligned to the G/A-rich portion of the *UPF3A* gene. The nucleotide sequence of the above gene portion and its corresponding amino acid sequence are presented below the browser panel. Reads are displayed as a bundle of lines above the corresponding covered sequences. Color dashes on these lines designate the positions of various mismatches in the reads. T/C transitions that appear as blue dashes are indicated by arrows. G/A-rich sequences with and without T-nucleotide insertions are shown in red ovals and marked with red curly brackets.

Codon content in mRNA regions cross-linked to ^{FLAG}uS19

Codons consisting of residues G and A encode Lys ($AA^A/_G$), Arg ($AG^A/_G$), Glu ($GA^A/_G$) and Gly ($GG^A/_G$). However, in the identified G/A-rich sequences, codons located at a distance up to 19 nucleotide triplets upstream and downstream of that in the ribosomal A site were represented mainly by Glu and Lys codons, while Arg codons were less common, and Gly codons were practically absent (Figure 6, Supplementary Table S3). The examination of the codon content in the above regions showed that Glu and Lys codons mostly alternated with each other periodically and irregularly, practically without forming of extended homomeric chains encoding more than 4 amino acid residues (Figure 6, Supplementary Table S3). Thus, mRNA regions, in which the frequent occurrence of Lys and, more rarely, Arg codons is accompanied with the frequent appearance of Glu codons, turned out to be efficiently cross-linked to ^{FLAG}uS19 via the A site s^4U-containing codon.

To find out whether the high frequency of the Glu and Lys/Arg codons in any mRNA region could provide cross-linking to ^{FLAG}uS19 in ribosomes stopped by cycloheximide, we attempted to estimate the presence of mRNAs that cross-linked to ^{FLAG}uS19 among mRNAs encoding proteins with the Glu/Lys irregular repeats. Considering the peptide motif $(E/K)_{12}$ as a reference, we extracted all human proteins with such motifs from the Ensembl database. Since the codons for Glu and Lys do not have a U residue and, therefore, are not able to cross-link to ^{FLAG}uS19 in s^4U-treated cells, when extracting the above proteins, we allowed up to 4 random substitutions in the motif $(E/K)_{12}$ sequence, so that it could include an amino acid whose codon comprises a U residue. The list of genes corresponding to

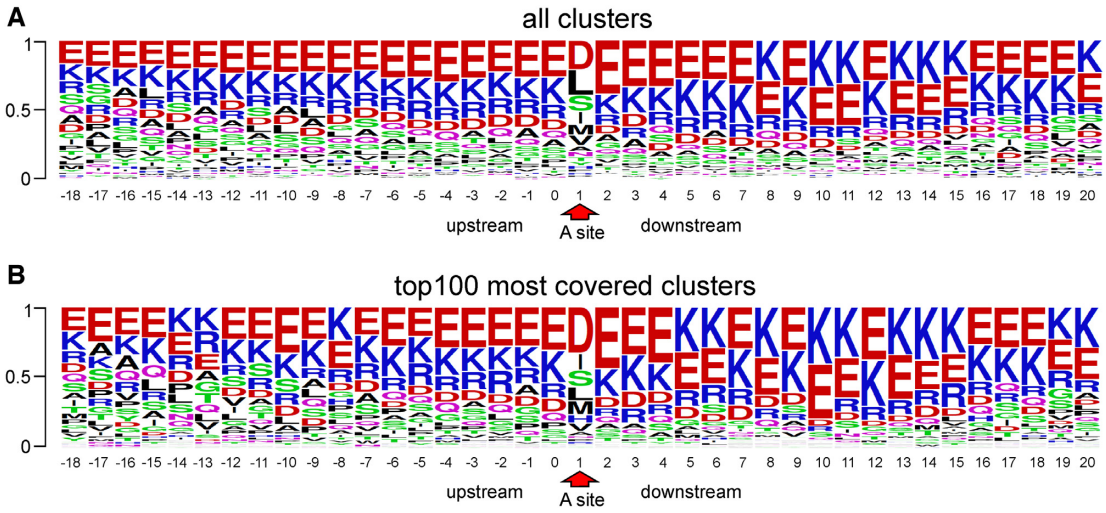

Figure 6. Logos of amino acid sequences corresponding to the nucleotide sequences presented as logos in Figure 4. The numbering of the amino acid positions is the same as in (39), where the position of the amino acid residue corresponding to the P-site-bound codon is designed as 0, and to the A site-bound codon as +1. (**A**) and (**B**), see legend to Figure 4.

the amino acid sequences derived in this way was then restricted to those that were among the top 1000 of genes with the highest read coverage, which have been identified using Ribo-seq data from HEK293 cells (37). Using this simple filter, we found 118 genes encoding proteins with the motifs $(E/K)_{12}$ and 51 of them turned out to be present in the set of genes corresponding to mRNAs cross-linked to ^{FLAG}uS19 (Supplementary Table S4). Thus, about half of cellular mRNAs encoding proteins with the Glu/Lys irregular repeats are those that are capable of cross-linking to ^{FLAG}uS19. A visual inspection of the remaining 67 genes in the IGV genome browser showed that many of them had clusters with T/C transitions. However, these clusters did not meet the criteria used to be selected as those that matched the cross-linked regions of mRNAs, because of either low read coverage or an insufficient number of T/C transitions, or the lack of appropriate T residues. Obviously, the incomplete correspondence between the compared sets of genes was due to strict criteria for the selection of clusters with T/C transitions and the simplicity of the chosen reference sequence. Therefore, ^{FLAG}uS19 cross-linking to the s^4U-containing codons within mRNA regions with a high frequency of Glu and Lys/Arg ones did not depend on the sequences of particular mRNAs, and was predetermined by the nature of the amino acid residues encoded by these regions.

DISCUSSION

In this study, the interaction of cellular mRNAs with the ribosomal protein uS19, whose C-terminal tail is known to be located at the decoding site of the 80S ribosome, was first unraveled at the translatome level using the PAR-CLIP method applied to a stable ^{FLAG}uS19-producing cell line. Our findings, based on the analysis of NGS-derived data, showed that in human ribosomes stalled by cycloheximide, ^{FLAG}uS19 efficiently cross-linked to mRNA regions with a high G/A content encoding amino acid residues Glu, Lys and, more rarely, Arg, without forming cross-links to any other regions.

As is known, the distinctive features of the above amino acid residues are their charge and bulkiness, and therefore a large number of these residues in the nascent polypeptide can interfere with its movement through the ribosomal tunnel, which starts at the peptidyl transferase center (PTC) (38,39). One of the functions of this tunnel is to ensure the unhindered exit of the newly synthesized polypeptide chain from the ribosome. At the same time, the data gained with bacterial ribosomes have shown that the tunnel walls, which are formed mainly by nucleotide residues of the large subunit rRNA (40,41), are involved in monitoring the amino acid sequence of the polypeptide passing along them (42). Moreover, the moving polypeptide can interact with the tunnel walls, which results in ribosome pausing at the respective mRNA region during translation elongation (reviewed in (43,44)). In addition, using a rabbit reticulocyte cell-free protein-synthesizing translation system, it has been found that chains of positively charged Arg and Lys residues, while in the ribosomal tunnel, could modulate the rate of translation elongation, leading to temporarily arrested ribosomes (45).

All of the above allowed us to conclude that when ^{FLAG}uS19-producing cells were treated with cycloheximide, some portion of the translating ribosomes was already paused at G/A-enriched regions in mRNA CDSs, which were identified as cross-linked to ^{FLAG}uS19. Hence, as expected, cycloheximide-arrested ribosomes were different types of complexes, including those, in which the A site codon was not involved in the formation of the mRNA-tRNA duplex and was accessible for interaction with ^{FLAG}uS19. It should be noted that in the aforementioned study (45) for the chain of negatively charged Glu residues, unlike those of Arg and Lys residues, no stopping of the ribosome has been observed. Therefore, one can assume that ribosome pausing detected in the current study is a consequence of a decrease in the rate of translation

elongation due to the alternation of side chains of negatively charged Glu residues with those of positively charged Lys/Arg ones in the nascent polypeptide. During translocation of peptidyl-tRNA, the alternation of the above residues might significantly complicate the passage of the peptidyl moiety from the A site to the P site on the large subunit. Accordingly, the state of peptidyl-tRNA in the paused ribosomes might be characterized as a hybrid P/A one. Alternatively, peptidyl-tRNA might be in the P/P-state, but rearrangements in PTC caused by the interaction of the ribosomal tunnel with a moving peptide did not allow aminoacyl-tRNA to enter the A site, and, as a result, a codon located at the decoding site was accessible for contact with the uS19 tail. The possibility of such rearrangements has been shown in cryo-EM studies of the structure of bacterial 70S paused ribosomes obtained using mRNAs encoding specific peptides that caused the arrest of translation (46,47). The lack of ^{FLAG}uS19 cross-linking sites in mRNA regions other than those mentioned above could be due to the shielding effect of peptidyl-tRNA, which was in the hybrid A/P state (48) in the remaining cycloheximide-arrested ribosomes, similar to the effect observed in our *in vitro* experiments on cross-linking of mRNAs II and III to human 80S ribosomes.

Thus, based on the obtained PAR-CLIP data, one can conclude that the mRNA codon entering the ribosomal A site interacts with the C-terminal tail of uS19 through its nucleotide base and that this tail becomes poorly accessible for this interaction at the subsequent stages of the elongation cycle when the A site is occupied by aminoacyl- or peptidyl-tRNA. However, experiments to examine the effect of the A-site tRNA *in vitro* show that it only partially protects uS19 from cross-linking to the A-site s^4U-containing codon. The disagreement between the protective effects of the A site tRNA observed in the *in vivo* translation system and the 'non-enzymatic' one is likely related to different binding ways of tRNA molecules in the ribosomal A site *in vivo* and *in vitro.* In the latter case, the cognate tRNA binds at the A site in a codon-dependent manner directly, without the initial recognition and accommodation steps required in a real translation system when aminoacyl-tRNA is delivered to the ribosome in the complex with eEF-1 and GTP. Accordingly, tRNA bound at the A site 'non-enzymatically' should be in equilibrium with free unbound tRNA, which was taken in excess over ribosomes to provide a higher level of the binding. Therefore, during irradiation, uS19 could cross-link to the s^4U-containing mRNA codon at the time when one tRNA was already dissociated from the A site and the other did not yet bind there. In contrast, in the *in vivo* translation system, the tRNA molecule bound at the A site cannot leave this site before transpeptidation and the subsequent translocation of the resulting peptidyl-tRNA from the A to the P site, which allows it to completely block the cross-linking of the s^4U-containing codon located at the A site to uS19.

Why does the ribosomal protein uS19 interact with mRNA at the decoding site during translation elongation? Considering that the uS19 tail is in contact with a stop codon in the pre-termination complex (4–7,49), one can suppose that the functional assignment of the occurrence of this tail in the decoding site is to ensure the proper location of the A site codon when it is recognized by cognate aminoacyl-tRNA or eRF1. The N-terminal fragment of the ribosomal protein eS30 most likely assists the uS19 tail in maintaining the A site codon conformation necessary for recognition, since it is also located in the decoding site (see Introduction) and its interaction with the A site codon is completely blocked by an A site-bound ligand (7,9). In this regard, it is obvious that results similar to those obtained with ^{FLAG}uS19-producing cells could be gained by applying the PAR-CLIP method to ^{FLAG}eS30-producing ones. However, so far we have no data to judge to which extent the interactions of these proteins with mRNAs are important for the decoding process and what happens if they do not occur. Determining whether the interactions of the C-terminal tail of uS19 and the N-terminal fragment of eS30 with mRNAs at the ribosomal decoding site are critical for elongation may be the next step in the investigation of the involvement of human ribosomal proteins in the translation process.

In general, the results of this study clearly show that the C-terminal tail of uS19 directly interacts with cellular mRNAs at the ribosomal A site. Since this interaction occurs only if the A site codon does not participate in the formation of the mRNA-tRNA duplex, the regions of cellular mRNAs involved in interaction with uS19 are actually those, at which ribosomes pause during translation elongation because of their inability to bind aminoacyl-tRNAs. These regions include sequences encoding protein portions rich in the amino acid residues Glu, Lys and Arg, which interfere with the movement of the growing polypeptide through the ribosomal tunnel. Thus, our findings shed light on previously unknown features of translation elongation in mammalian cells, allowing a fresh look at this process.

DATA AVAILABILITY

The read data reported in this study were deposited in the GEO under the accession number GSE128265.

SUPPLEMENTARY DATA

Supplementary Data are available at NAR Online.

ACKNOWLEDGEMENTS

The authors are grateful to SB RAS Genomics Core Facility for the sequencing.

FUNDING

Russian Foundation for Basic Research [17-04-00609 to G.G.K.]; Russian state funded budget of ICBFM SB RAS [project AAAA-A17-117020210022-4]; Russian Ministry of Science and Higher Education under 5-100 Excellence Programme. Funding for open access charge: Russian Foundation for Basic Research.
Conflict of interest statement. None declared.

REFERENCES

1. Graifer,D. and Karpova,G. (2018) The interaction of mRNA with ribosomes in the course of translation in higher eukaryotes. In:

Fernandez,I and Jackson,L (eds). *mRNA: Molecular Biology, Processing and Function*. Nova Science Publishers, Inc., NY, pp. 1–42.
2. Graifer,D. and Karpova,G. (2015) Roles of ribosomal proteins in the functioning of translational machinery of eukaryotes. *Biochimie*, **109**, 1–17.
3. Ban,N., Beckmann,R., Cate,J.H., Dinman,J.D., Dragon,F., Ellis,S.R., Lafontaine,D.L., Lindahl,L., Liljas,A., Lipton,J.M. *et al.* (2014) A new system for naming ribosomal proteins. *Curr. Opin. Struc. Biol.*, **24**, 165–169.
4. Chavatte,L., Frolova,L., Kisselev,L. and Favre,A. (2001) The polypeptide chain release factor eRF1 specifically contacts the s(4)UGA stop codon located in the A site of eukaryotic ribosomes. *Eur. J. Biochem.*, **268**, 2896–2904.
5. Chavatte,L., Seit-Nebi,A., Dubovaya,V. and Favre,A. (2002) The invariant uridine of stop codons contacts the conserved NIKSR loop of human eRF1 in the ribosome. *EMBO J.*, **21**, 5302–5311.
6. Chavatte,L., Frolova,L., Laugaa,P., Kisselev,L. and Favre,A. (2003) Stop codons and UGG promote efficient binding of the polypeptide release factor eRF1 to the ribosomal A site. *J. Mol. Biol.*, **331**, 745–758.
7. Bulygin,K., Chavatte,L., Frolova,L., Karpova,G. and Favre,A. (2005) The first position of a codon placed in the A site of the human 80S ribosome contacts nucleotide C1696 of the 18S rRNA as well as proteins S2, S3, S3a, S30, and S15. *Biochemistry*, **44**, 2153–2162.
8. Graifer,D., Molotkov,M., Styazhkina,V., Demeshkina,N., Bulygin,K., Eremina,A., Ivanov,A., Laletina,E., Ven'yaminova,A. and Karpova,G. (2004) Variable and conserved elements of human ribosomes surrounding the mRNA at the decoding and upstream sites. *Nucleic Acids Res.*, **32**, 3282–3293.
9. Molotkov,M.V., Graifer,D.M., Popugaeva,E.A., Bulygin,K.N., Meschaninova,M.I., Ven'yaminova,A.G. and Karpova,G.G. (2006) mRNA 3′ of the A site bound codon is located close to protein S3 on the human 80S ribosome. *RNA Biol.*, **3**, 122–129.
10. Pisarev,A.V., Kolupaeva,V.G., Pisareva,V.P., Merrick,W.C., Hellen,C.U. and Pestova,T.V. (2006) Specific functional interactions of nucleotides at key −3 and +4 positions flanking the initiation codon with components of the mammalian 48S translation initiation complex. *Genes Dev.*, **20**, 624–636.
11. Pisarev,A.V., Kolupaeva,V.G., Yusupov,M.M., Hellen,C.U. and Pestova,T.V. (2008) Ribosomal position and contacts of mRNA in eukaryotic translation initiation complexes. *EMBO J.*, **27**, 1609–1621.
12. Sharifulin,D.E., Grosheva,A.S., Bartuli,Y.S., Malygin,A.A., Meschaninova,M.I., Ven'yaminova,A.G., Stahl,J., Graifer,D.M. and Karpova,G.G. (2015) Molecular contacts of ribose-phosphate backbone of mRNA with human ribosome. *Biochim. Biophys. Acta*, **1849**, 930–939.
13. Budkevich,T.V., Giesebrecht,J., Behrmann,E., Loerke,J., Ramrath,D.J., Mielke,T., Ismer,J., Hildebrand,P.W., Tung,C.S., Nierhaus,K.H. *et al.* (2014) Regulation of the mammalian elongation cycle by subunit rolling: a eukaryotic-specific ribosome rearrangement. *Cell*, **158**, 121–131.
14. Bulygin,K.N., Graifer,D.M., Hountondji,C., Frolova,L.Y. and Karpova,G.G. (2017) Exploring contacts of eRF1 with the 3′-terminus of the P site tRNA and mRNA stop signal in the human ribosome at various translation termination steps. *Biochim. Biophys. Acta*, **1860**, 782–793.
15. Khairulina,J., Graifer,D., Bulygin,K., Ven'yaminova,A., Frolova,L. and Karpova,G. (2010) Eukaryote-specific motif of ribosomal protein S15 neighbors A site codon during elongation and termination of translation. *Biochimie*, **92**, 820–825.
16. Shao,S., Murray,J., Brown,A., Taunton,J., Ramakrishnan,V. and Hegde,R.S. (2016) Decoding mammalian ribosome-mRNA states by translational GTPase complexes. *Cell*, **167**, 1229–1240.
17. Garreau de Loubresse,N., Prokhorova,I., Holtkamp,W., Rodnina,M.V., Yusupova,G. and Yusupov,M. (2014) Structural basis for the inhibition of the eukaryotic ribosome. *Nature*, **513**, 517–522.
18. Myasnikov,A.G., Kundhavai Natchiar,S., Nebout,M., Hazemann,I., Imbert,V., Khatter,H., Peyron,J.F. and Klaholz,B.P. (2016) Structure-function insights reveal the human ribosome as a cancer target for antibiotics. *Nat. Commun.*, **7**, 12856.
19. Schneider-Poetsch,T., Ju,J., Eyler,D.E., Dang,Y., Bhat,S., Merrick,W.C., Green,R., Shen,B. and Liu,J.O. (2010) Inhibition of eukaryotic translation elongation by cycloheximide and lactimidomycin. *Nat. Chem. Biol.*, **6**, 209–217.
20. Buskirk,A.R. and Green,R. (2017) Ribosome pausing, arrest and rescue in bacteria and eukaryotes. *Phil. Trans. R. Soc. B*, **372**, 20160183.
21. Joazeiro,C.A.P. (2017) Ribosomal stalling during translation: providing substrates for ribosome-associated protein quality control. *Annu. Rev. Cell Dev. Biol.*, **33**, 343–368.
22. Hafner,M., Landthaler,M., Burger,L., Khorshid,M., Hausser,J., Berninger,P., Rothballer,A., Ascano,M. Jr., Jungkamp,A.C., Munschauer,M. *et al.* (2010) Transcriptome-wide identification of RNA-binding protein and microRNA target sites by PAR-CLIP. *Cell*, **141**, 129–141.
23. Matasova,N.B., Myltseva,S.V., Zenkova,M.A., Graifer,D.M., Vladimirov,S.N. and Karpova,G.G. (1991) Isolation of ribosomal subunits containing intact rRNA from human placenta: estimation of functional activity of 80S ribosomes. *Anal. Biochem.*, **198**, 219–223.
24. Bulygin,K.N., Bartuli,Y.S., Malygin,A.A., Graifer,D.M., Frolova,L.Y. and Karpova,G.G. (2016) Chemical footprinting reveals conformational changes of 18S and 28S rRNAs at different steps of translation termination on the human ribosome. *RNA*, **22**, 278–289.
25. Malygin,A.A., Kossinova,O.A., Shatsky,I.N. and Karpova,G.G. (2013) HCV IRES interacts with the 18S rRNA to activate the 40S ribosome for subsequent steps of translation initiation. *Nucleic Acids Res.*, **41** 8706–8714.
26. Gopanenko,A.V., Malygin,A.A., Tupikin,A.E., Laktionov,P.P., Kabilov,M.R. and Karpova,G.G. (2017) Human ribosomal protein eS1 is engaged in cellular events related to processing and functioning of U11 snRNA. *Nucleic Acids Res.*, **45**, 9121–9137.
27. Kargapolova,Y., Levin,M., Lackner,K. and Danckwardt,S. (2017) sCLIP-an integrated platform to study RNA-protein interactomes in biomedical research: identification of CSTF2tau in alternative processing of small nuclear RNAs. *Nucleic Acids Res.*, **45**, 6074–6086.
28. Hashimshony,T., Senderovich,N., Avital,G., Klochendler,A., de Leeuw,Y., Anavy,L., Gennert,D., Li,S., Livak,K.J., Rozenblatt-Rosen,O. *et al.* (2016) CEL-Seq2: sensitive highly-multiplexed single-cell RNA-Seq. *Genome Biol.*, **17**, 77.
29. Dobin,A., Davis,C.A., Schlesinger,F., Drenkow,J., Zaleski,C., Jha,S., Batut,P., Chaisson,M. and Gingeras,T.R. (2013) STAR: ultrafast universal RNA-seq aligner. *Bioinformatics*, **29**, 15–21.
30. Smith,T., Heger,A. and Sudbery,I. (2017) UMI-tools: modeling sequencing errors in Unique Molecular Identifiers to improve quantification accuracy. *Genome Res.*, **27**, 491–499.
31. Durinck,S., Spellman,P.T., Birney,E. and Huber,W. (2009) Mapping identifiers for the integration of genomic datasets with the R/Bioconductor package biomaRt. *Nat. Protoc.*, **4**, 1184–1191.
32. Lawrence,M., Huber,W., Pages,H., Aboyoun,P., Carlson,M., Gentleman,R., Morgan,M.T. and Carey,V.J. (2013) Software for computing and annotating genomic ranges. *PLoS Comput. Biol.*, **9**, e1003118.
33. Ingolia,N.T., Brar,G.A., Rouskin,S., McGeachy,A.M. and Weissman,J.S. (2012) The ribosome profiling strategy for monitoring translation in vivo by deep sequencing of ribosome-protected mRNA fragments. *Nat. Protoc.*, **7**, 1534–1550.
34. Ingolia,N.T., Lareau,L.F. and Weissman,J.S. (2011) Ribosome profiling of mouse embryonic stem cells reveals the complexity and dynamics of mammalian proteomes. *Cell*, **147**, 789–802.
35. Ingolia,N.T., Ghaemmaghami,S., Newman,J.R. and Weissman,J.S. (2009) Genome-wide analysis in vivo of translation with nucleotide resolution using ribosome profiling. *Science*, **324**, 218–223.
36. Steitz,J.A. (1969) Polypeptide chain initiation: nucleotide sequences of the three ribosomal binding sites in bacteriophage R17 RNA. *Nature*, **224**, 957–964.
37. Li,X., Xiong,X., Zhang,M., Wang,K., Chen,Y., Zhou,J., Mao,Y., Lv,J., Yi,D., Chen,X.W. *et al.* (2017) Base-resolution mapping reveals distinct m(1)A methylome in nuclear- and mitochondrial-encoded transcripts. *Mol. Cell*, **68**, 993–1005.
38. Kosolapov,A. and Deutsch,C. (2009) Tertiary interactions within the ribosomal exit tunnel. *Nat. Struct. Mol. Biol.*, **16**, 405–411.
39. Mankin,A.S. (2006) Nascent peptide in the "birth canal" of the ribosome. *Trends Biochem. Sci.*, **31**, 11–13.
40. Ban,N., Nissen,P., Hansen,J., Moore,P.B. and Steitz,T.A. (2000) The complete atomic structure of the large ribosomal subunit at 2.4 A resolution. *Science*, **289**, 905–920.
41. Harms,J., Schluenzen,F., Zarivach,R., Bashan,A., Gat,S., Agmon,I., Bartels,H., Franceschi,F. and Yonath,A. (2001) High resolution

structure of the large ribosomal subunit from a mesophilic eubacterium. *Cell*, **107**, 679–688.
42. Martinez,A.K., Shirole,N.H., Murakami,S., Benedik,M.J., Sachs,M.S. and Cruz-Vera,L.R. (2012) Crucial elements that maintain the interactions between the regulatory TnaC peptide and the ribosome exit tunnel responsible for Trp inhibition of ribosome function. *Nucleic Acids Res.*, **40**, 2247–2257.
43. Ito,K. and Chiba,S. (2013) Arrest peptides: cis-acting modulators of translation. *Annu. Rev. Biochem.*, **82**, 171–202.
44. Wilson,D.N., Arenz,S. and Beckmann,R. (2016) Translation regulation via nascent polypeptide-mediated ribosome stalling. *Curr. Opin. Struc. Biol.*, **37**, 123–133.
45. Lu,J. and Deutsch,C. (2008) Electrostatics in the ribosomal tunnel modulate chain elongation rates. *J. Mol. Biol.*, **384**, 73–86.
46. Sohmen,D., Chiba,S., Shimokawa-Chiba,N., Innis,C.A., Berninghausen,O., Beckmann,R., Ito,K. and Wilson,D.N. (2015) Structure of the Bacillus subtilis 70S ribosome reveals the basis for species-specific stalling. *Nat. Commun.*, **6**, 6941.
47. Zhang,J., Pan,X., Yan,K., Sun,S., Gao,N. and Sui,S.F. (2015) Mechanisms of ribosome stalling by SecM at multiple elongation steps. *eLife*, **4**, e09684.
48. Julian,P., Konevega,A.L., Scheres,S.H., Lazaro,M., Gil,D., Wintermeyer,W., Rodnina,M.V. and Valle,M. (2008) Structure of ratcheted ribosomes with tRNAs in hybrid states. *Proc. Natl. Acad. Sci. U.S.A.*, **105**, 16924–16927.
49. Bulygin,K.N., Khairulina,Y.S., Kolosov,P.M., Ven'yaminova,A.G., Graifer,D.M., Vorobjev,Y.N., Frolova,L.Y. and Karpova,G.G. (2011) Adenine and guanine recognition of stop codon is mediated by different N domain conformations of translation termination factor eRF1. *Nucleic Acids Res.*, **39**, 7134–7146.